Linear processes that produce $1/f$ or flicker noise

Edoardo Milotti
Dipartimento di Fisica dell'Universitá di Trieste, Via Valerio 2, I-34127 Trieste, Italy
and Istituto Nazionale di Fisica Nucleare, Sezione di Trieste Via Valerio 2, I-34127 Trieste, Italy
(Received 14 June 1994; revised manuscript received 19 December 1994)

$1/f$ noise and flicker noises — i.e., the class of $1/f^{\alpha}$ noises with $0.5 < \alpha < 0.5$—are as ubiquitous as they are mysterious. Several physical mechanisms to generate $1/f$ noise have been devised, and most of them try to obtain a broad, nearly flat distribution of relaxation times, which would then yield a $1/f$ spectrum. However, they are all very specialized, and none of them addresses the question of the apparent universality of this noise, while they all fail in some respect. I show here that the power spectral density of a relaxing linear system driven by white noise is determined by the eigenvalue density of the linear operator associated with the system. I also show that the eigenvalue densities of linear operators that describe diffusion and transport lead to $1/f$ or flicker noise. Using the concepts developed in the paper and a rough approximation of transport in a resistor, I derive the Hooge formula for the spectrum of conductance fluctuations.

PACS number(s): 02.50.Ey, 05.40.+j, 05.60.+w

I. INTRODUCTION

$1/f$ noise appears again and again in many apparently uncorrelated systems as diverse as metal-oxide-semiconductor (MOS) devices and ocean currents [1–4]. Indeed there are models that justify the occurrence of $1/f$ noise in some systems (see the reviews [5–7]), but they are very specialized, in other words they do not have the "universality" suggested by the ubiquity of $1/f$ noise. It is generally accepted that the mechanism that leads to $1/f$ noise is a system with an exponential response function driven by a shot noise source, and such that the relaxation times of the system are chosen at random from a very broad, flat distribution. The power spectral density (PSD) of a simple relaxation process with characteristic time τ and rate $\lambda = 1/\tau$ is proportional to $1/(\omega^2+\lambda^2)$ (ω is the angular frequency), and if the rates are uniformly distributed between the limits $\lambda_{\min}$ and $\lambda_{\max}$, then the PSD is given by the integral

$$S(\omega) \propto \int_{\lambda_{\min}}^{\lambda_{\max}} \frac{d\lambda}{\omega^2+\lambda^2} = \frac{1}{\omega}\left(\arctan\frac{\lambda_{\max}}{\omega} - \arctan\frac{\lambda_{\min}}{\omega}\right). \quad (1)$$

Then if $\lambda_{\min} \ll \omega \ll \lambda_{\max}$, $S(\omega) \propto 1/\omega$, and thus a flat distribution yields a $1/f$ spectrum. Furthermore such a distribution gives a stationary Gaussian process if the driving noise source is itself stationary and Gaussian, and this agrees well with most experimental observations of the statistical properties of $1/f$ noise, and also seems to rule out all explanations that relate this noise to some underlying nonlinear dynamics. However, as Press puts it in his nice review paper [1], "it [is] hard to conceive ... physical mechanisms which contribute stretched pulses with just the right frequency of occurrence over, say, six orders of magnitude. Scale superposition just transfers the mystery to the random 'stretching factor' process." I suggest here a fairly general explanation which depends only on very weak assumptions: the PSD of a linear system [8] driven by white Gaussian noise is uniquely determined by the eigenvalue density of the associated linear operator, and the (linear) operators that describe several systems that exhibit flicker noise, and in particular diffusion and transport, have densities that lead to $1/f$ or flicker noise— i.e., to $1/f^{\alpha}$ noises with $0.5 < \alpha < 1.5$. This is a purely mathematical device that does not depend on the underlying physics, and there is no need to introduce a "stretching factor." Although the mathematics developed here is applicable to many systems that are totally unrelated to $1/f$ current noise, the main application of a flicker noise theory is the "explanation" of $1/f$ current noise. This requires a description of charge transport and diffusion, and here I make an attempt to go in this direction, but I do not develop a complete theory of flicker noise in resistors. It must be remarked that diffusion processes have been repeatedly invoked as the source of $1/f$ noise in resistors, most notably by Voss and Clark [9], who have introduced a diffusion model based on temperature fluctuations. The model described in this paper is based on number fluctuations — and therefore has a much wider applicability — and goes further in the analysis thanks to a considerably simpler mathematical formalism.

Section II outlines the connection between diffusion, transport, and systems of linear differential equations of the relaxation type. The PSD is discussed in Sec. III, while in Sec. IV I return to the description of Sec. II and derive lower and upper bounds for the eigenvalues. Section V exhibits classes of processes that actually convert white noise to $1/f$ or flicker noise. A simple transport channel that may roughly model a resistor is described in Sec.VI, and it is shown that this model leads to the Hooge formula for conductance fluctuations. Notice that no special distinction is made, throughout the paper, between "equilibrium" and "transport" noise.

II. DIFFUSION AND TRANSPORT PROCESSES ON A DISCRETE SET OF SITES

Several measurements [5–7,9] indicate that $1/f$ noise in resistors exists at equilibrium, and therefore that it may be due to some sort of diffusion. Thus we start here with pure diffusion and consider a population of N identical noninteracting random walkers distributed over n sites, so that $N_k(t)$ is the population of the kth site at time t, and $a_{kj}\Delta t$ is the probability that a random walker which is at site j jumps to site k during the (short) time interval $(t, t+\Delta t)$. At present no special topology is associated with the n sites, however we make the additional hypothesis $N \gg n$; as we shall see later this is not a serious restriction.

Then the number of random walkers that jump from site j to site k during $(t, t+\Delta t)$ is a random variable with a binomial distribution, with average and variance both equal to $a_{kj}N_j(t)\Delta t$. It is well known from elementary probability theory [10] that if $a_{kj}N_j(t)\Delta t$ is finite and large then such a binomial distribution can be approximated by a Gaussian density with the same average and variance. The total number of random walkers that jump to k is then (in the limit of large N_j) a sum of independent Gaussian variates, and therefore it is itself a Gaussian variate with average and variance both equal to

$$\sum_{\substack{j=1,n\\ j\neq k}} a_{kj}N_j(t)\Delta t, \tag{2}$$

while the total number of random walkers that jump *away* from site k during the same time interval is still another Gaussian variate with average and variance both equal to

$$\sum_{\substack{j=1,n\\ j\neq k}} a_{jk}N_k(t)\Delta t = N_k(t)\sum_{\substack{j=1,n\\ j\neq k}} a_{jk}dt = \frac{1}{\tau_k}N_k(t)\Delta t, \tag{3}$$

thus the net change of the population $N_k(t)$ during the time interval $(t, t+\Delta t)$ is

$$\Delta N_k = -\frac{1}{\tau_k}N_k(t)\Delta t + \sum_{\substack{j=1,n\\ j\neq k}} a_{kj}N_j(t)\Delta t + \nu_k(t)\Delta t. \tag{4}$$

The previous considerations suggest that each ν_k can be well approximated by a Gaussian noise process and in addition we *assume* that the ν_k's are uncorrelated from each other, so that these noises are completely described by

$$\langle \nu_k(t)\rangle = 0, \tag{5a}$$

$$\langle \nu_j(t)\nu_k(t')\rangle = \sigma_k^2\delta_{jk}\delta(t-t'), \tag{5b}$$

$$\sigma_k^2 = \sum_{\substack{j=1,n\\ j\neq k}} a_{kj}N_j(t) + \sum_{\substack{j=1,n\\ j\neq k}} a_{jk}N_k(t) \approx \sum_{\substack{j=1,n\\ j\neq k}} (a_{kj}\langle N_j\rangle + a_{jk}\langle N_k\rangle) \tag{5c}$$

(here $\langle\cdots\rangle$ denotes the ensemble average).

Notice that the global condition $\sum_{k=1}^{n}\Delta N_k = 0$ should also hold (i.e., the total number of random walkers is conserved), therefore (5b) can be only approximately true. However, this global condition becomes less and less important as n grows (because the residual correlation is spread out over a very large number of variates), and disappears in the more realistic models that we shall introduce in Sec. IV, therefore we assume (5b) from the outset. Another potential problem with ν_k's are the long tails of its assumed Gaussian density, which may lead to negative occupation numbers and thus to large negative population changes, so that in practice one has to require the additional condition $-\Delta N_k \leq N_k$. Since (5c) defines a Gaussian density with $\sigma_k/\langle N_k\rangle \sim 1/\sqrt{N_k}$, we expect the tails to be negligible for large N_k, and thus we expect that the condition $-\Delta N_k \leq N_k$ is obeyed by the Gaussian density with a probability that approaches 1 for large N_k, so that the Gaussian hypothesis does not adversely affect the PSD. In Sec. V, with the aid of computer simulations, it will be shown that it is actually so (see also note [11]).

Introducing the vectors $\boldsymbol{N} = \{N_k\}_{k=1,\ldots,n}$, $\boldsymbol{\nu} = \{\nu_k\}_{k=1,\ldots,n}$ and the matrix $A = \{a_{jk}\}_{j,k=1,\ldots,n}$ with $a_{kk} = -\frac{1}{\tau_k}$, we can rewrite Eq. (4) in vector form:

$$d\boldsymbol{N} = A\boldsymbol{N}dt + \boldsymbol{\nu}dt. \tag{6}$$

Now assume that the sites $1,\ldots,n$ are chained together so that site k is adjacent to sites $k-1$ and $k+1$. Then ordinary diffusion due to the simple one-dimensional (1D) unbiased random walk can be recovered if we let $n\to\infty$, $a_{jj} = -\frac{1}{\tau}$, $a_{k,k\pm1} = \frac{1}{2\tau}$, and $a_{jk} = 0$ if $j \neq k, k\pm1$. In fact from definition (3), τ_k is given by $\tau_k = (a_{k-1,k}+a_{k+1,k})^{-1}$ and therefore $\tau_k = \tau$ is the same for all k's, and

$$dN_k = -\frac{1}{\tau}N_k(t)dt + \frac{1}{2\tau}[N_{k+1}(t) + N_{k-1}(t)]dt + \nu_k(t)dt. \tag{7}$$

Then taking the ensemble average, introducing the position variable $x = k\Delta x$, and denoting $N(x,t) = \langle N_k(t)\rangle$, where Δx is the (small) distance between adjacent sites, we find

$$dN(x,t) = -\frac{1}{\tau}N(x,t)dt + \frac{1}{2\tau}[N(x+\Delta x,t) + N(x-\Delta x,t)]dt. \tag{8}$$

Eventually, if Δx is very small we can write

$$\frac{\partial N}{\partial t} = \frac{1}{2}D\frac{\partial^2 N}{\partial t^2}, \tag{9}$$

where $D = \Delta x^2/\tau$ is the diffusion constant, and this is just the usual forward Fokker-Planck equation [for the average values $N(x,t)$] for the simple random walk (see, e.g., [10]).

Similarly if we take the same topology and let $a_{jj} = -\frac{1}{\tau}$, $a_{j,j-1} = \frac{p}{\tau}$, $a_{j,j+1} = \frac{q}{\tau}$ with $p+q=1$, $p,q\geq 0$, and $a_{jk} = 0$ if $j \neq k\pm1$, we recover the forward Fokker-Planck equation for diffusion + transport (i.e., for the

biased 1D simple random walk, see also Ref. [10]),

$$\frac{\partial N}{\partial t} = \frac{1}{2}D\frac{\partial^2 N}{\partial t^2} - v\frac{\partial N}{\partial x} \tag{10}$$

with drift speed $v = (p-q)\Delta x/\tau$ and the same diffusion constant D as before.

III. POWER SPECTRAL DENSITIES

We introduce now the spectral representations for the populations and for the noise processes:

$$N_k(t) = \frac{1}{2\pi}\int_{-\infty}^{+\infty} e^{i\omega t}F_k(\omega)d\omega, \tag{11}$$

$$\nu_k(t) = \frac{1}{2\pi}\int_{-\infty}^{+\infty} e^{i\omega t}f_k(\omega)d\omega. \tag{12}$$

Then, proceeding as in [12] and using Eq. (6), we can write

$$i\omega \boldsymbol{F}(\omega) = A\boldsymbol{F}(\omega) + \boldsymbol{f}(\omega), \tag{13}$$

where $\boldsymbol{F}(\omega)=\{F_k(\omega)\}_{k=1,\ldots,n}$ and $\boldsymbol{f}(\omega)=\{f_k(\omega)\}_{k=1,\ldots,n}$ are the vectors of Fourier transforms. The last equation can be solved formally for $\boldsymbol{F}(\omega)$, and we find

$$\boldsymbol{F}(\omega) = (i\omega\mathbb{1} - A)^{-1}\boldsymbol{f}(\omega) \tag{14}$$

($\mathbb{1}$ is the identity matrix) so that, using the definition given in [13], the PSD of the stochastic process $N_k(t)$ is

$$\begin{aligned} S_k(\omega) &= \lim_{T\to\infty}\frac{\langle|F_k(\omega)|^2\rangle}{2\pi T} \\ &= \lim_{T\to\infty}\frac{\left\langle\left|\sum_{j=1}^{n}(i\omega\mathbb{1} - A)^{-1}_{kj}f_j(\omega)\right|^2\right\rangle}{2\pi T}. \end{aligned} \tag{15}$$

From the independence of the stochastic processes $\{\nu_k\}$ it follows that

$$S_k(\omega) = \sum_{j=1}^{n}|(i\omega\mathbb{1} - A)^{-1}_{kj}|^2\lim_{T\to\infty}\frac{\langle|f_j(\omega)|^2\rangle}{2\pi T}, \tag{16}$$

$$= \sum_{j=1}^{n}|(i\omega\mathbb{1} - A)^{-1}_{kj}|^2 s_j(\omega), \tag{17}$$

where $s_j(\omega)$ is the power spectral density of ν_j, i.e., $s_j(\omega) = \sigma_j^2/2\pi$.

Formally this solves the problem of finding the PSD. To proceed further we must make assumptions on the PSD's of the individual noise processes that drive the system. Since we are mostly concerned with noise in uniform systems, we assume that all the PSD's are the same, i.e., $\sigma_j^2 = \sigma^2$ for all j. We also assume that $a_{jk} = a_{kj}$ (i.e., the interaction between different sites is symmetric) and that the eigenvalues of A are not degenerate. Then the eigenvalues $\{\lambda_k\}_{k=1,\ldots,n}$ of A are real and there is an orthonormal basis of real eigenvectors $\{\boldsymbol{\eta}_k\}_{k=1,\ldots,n}$ such that $A\boldsymbol{\eta}_k = \lambda_k\boldsymbol{\eta}_k$. Using this basis we can write

$$\boldsymbol{F}(\omega) = \sum_{k=1}^{n}\Gamma_k(\omega)\boldsymbol{\eta}_k, \tag{18}$$

$$\boldsymbol{f}(\omega) = \sum_{k=1}^{n}\gamma_k(\omega)\boldsymbol{\eta}_k, \tag{19}$$

and substituting in Eq. (13) we obtain

$$\sum_{k=1}^{n}(i\omega - \lambda_k)\Gamma_k(\omega)\boldsymbol{\eta}_k = \sum_{k=1}^{n}\gamma_k(\omega)\boldsymbol{\eta}_k. \tag{20}$$

Because of the orthogonality of $\{\boldsymbol{\eta}_k\}$, equality holds for each component, i.e.,

$$\Gamma_k(\omega) = \frac{\gamma_k(\omega)}{(i\omega - \lambda_k)}, \tag{21}$$

and therefore

$$F_k(\omega) = \sum_{j=1}^{n}\frac{\gamma_j(\omega)}{(i\omega - \lambda_j)}(\boldsymbol{\eta}_j)_k. \tag{22}$$

The PSD is proportional to

$$\begin{aligned} \langle|F_k(\omega)|^2\rangle &= \left\langle\left|\sum_{j=1}^{n}\frac{\gamma_j(\omega)}{(i\omega - \lambda_j)}(\boldsymbol{\eta}_j)_k\right|^2\right\rangle \\ &= \sum_{j=1}^{n}\frac{\langle|\gamma_j|^2\rangle}{\omega^2 + \lambda_j^2}|(\boldsymbol{\eta}_j)_k|^2 \\ &\quad + \sum_{\substack{j,l \\ j\neq l}}\frac{\langle\gamma_j\gamma_l^*\rangle}{(i\omega + \lambda_j)(-i\omega + \lambda_l)}(\boldsymbol{\eta}_j)_k(\boldsymbol{\eta}_l^*)_k, \end{aligned} \tag{23}$$

and similarly

$$\begin{aligned} \langle|f_k(\omega)|^2\rangle &= \left\langle\left|\sum_{j=1}^{n}\gamma_j(\omega)(\boldsymbol{\eta}_j)_k\right|^2\right\rangle \\ &= \sum_{j=1}^{n}\langle|\gamma_j|^2\rangle|(\boldsymbol{\eta}_j)_k|^2 \\ &\quad + \sum_{\substack{j,l \\ j\neq l}}\langle\gamma_j\gamma_l^*\rangle(\boldsymbol{\eta}_j)_k(\boldsymbol{\eta}_l^*)_k. \end{aligned} \tag{24}$$

We have already assumed that at each site a random walker sees the same average environment, i.e., $\sigma_k = \sigma$ for all k's. Then both the vector $\boldsymbol{\nu}$ and the vectors of Fourier transforms $\boldsymbol{f}(\omega)$ are distributed with spherical symmetry in their n-dimensional spaces, and a rotation does not change the symmetry properties of the distributions. Therefore using $\{\boldsymbol{\eta}_k\}$ as a basis the stochastic processes $\{\gamma_k\}$ are still independent in the sense that $\langle\gamma_j^*(\omega)\gamma_k(\omega')\rangle = 0$ if $j \neq k$ and $\omega \neq \omega'$, and $\langle|\gamma_j(\omega)|^2\rangle = \langle|f_k(\omega)|^2\rangle$ for all j, k. Now we make use of the normalization conditions for the vectors, $\boldsymbol{\eta}_k$, i.e.,

$\sum_{j=1}^{n}|(\boldsymbol{\eta}_k)_j|^2=1$, and assume a uniform distribution of the eigenvector directions so that $\int_{\lambda_0}^{\lambda_0+\Delta\lambda}|[\boldsymbol{\eta}(\lambda)]_k|^2d\lambda\approx\Delta\lambda/n$. Then Eq. (23) becomes

$$\langle|F(\omega)|^2\rangle=\langle|F_k(\omega)|^2\rangle=\sum_{j=1}^{n}\frac{\langle|\gamma_j|^2\rangle}{\omega^2+\lambda_j^2}|(\boldsymbol{\eta}_j)_k|^2$$
$$\approx\langle|\gamma(\omega)|^2\rangle\int_{\lambda_{\min}}^{\lambda_{\max}}\frac{f_A(\lambda)}{\omega^2+\lambda^2}d\lambda, \tag{25}$$

where we have dropped the index k, since now all the spectral densities are the same, and where $\lambda_{\min}$ and $\lambda_{\max}$ are the minimum and maximum eigenvalues, and $f_A(\lambda)$ is the eigenvalue density of the matrix A, normalized so that $\int_{\lambda_{\min}}^{\lambda_{\max}}f_A(\lambda)d\lambda=1$. Moreover $s_j(\omega)=\sigma^2/2\pi$ and we get eventually

$$S(\omega)=\frac{\sigma^2}{2\pi n}\sum_{j=1}^{n}\frac{1}{\omega^2+\lambda_j^2}, \tag{26}$$
$$\approx\frac{\sigma^2}{2\pi}\int_{\lambda_{\min}}^{\lambda_{\max}}\frac{f_A(\lambda)}{\omega^2+\lambda^2}d\lambda. \tag{27}$$

Thus the shape of the spectrum $S(\omega)$ is determined by the eigenvalue density $f_A(\lambda)$ of the matrix A, and if it is nearly constant in the interval (λ_a,λ_b) (with $\lambda_a\ll\lambda_b$), then $S(\omega)$ has a $1/f$ dependence in the region $\lambda_a\ll\omega\ll\lambda_b$. (A different derivation and an extension of these results to the case of transport are given in Appendix A.)

IV. LOWER AND UPPER BOUNDS

We use now the Perron and the Gershgorin theorems to derive lower and upper bounds for the eigenvalues of the relaxation matrices introduced in Sec. II. These matrices have the general form

$$A=\begin{pmatrix}-\frac{1}{\tau_1} & a_{12} & a_{13} & \cdots\\ a_{21} & -\frac{1}{\tau_2} & a_{23} & \cdots\\ a_{31} & a_{32} & -\frac{1}{\tau_3} & \cdots\\ \vdots & \vdots & \vdots & \ddots\end{pmatrix} \tag{28}$$

with negative diagonal elements, while all nondiagonal elements are non-negative. We define first the matrix $A'=A+\frac{1}{\tau_{\min}}\mathbb{1}$, where $\tau_{\min}=\min_k\{\tau_k\}$, so that A' and A share the same eigenvectors, while the eigenvalues are shifted:

$$A'\boldsymbol{\eta}_k=\left(A+\frac{1}{\tau_{\min}}\mathbb{1}\right)\boldsymbol{\eta}_k=\left(\lambda_k+\frac{1}{\tau_{\min}}\right)\boldsymbol{\eta}_k=\lambda'_k\boldsymbol{\eta}_k. \tag{29}$$

Now A' is a non-negative matrix and the Perron theorem applies [14], with the result that there is a real eigenvalue $\lambda'_{\max}$ such that for any other eigenvalue α' of A' the inequality $|\alpha'|<\lambda'_{\max}$ holds, and $\lambda'_{\max}$ satisfies the following inequality:

$$\lambda'_{\max}\le\max_k\left\{\sum_{j=1}^{n}a'_{jk}\right\}$$
$$=\max_k\left\{\frac{1}{\tau_{\min}}-\frac{1}{\tau_k}+\sum_{\substack{j=1,n\\ j\neq k}}a_{jk}\right\}$$
$$=\frac{1}{\tau_{\min}}. \tag{30}$$

The inequality for the corresponding eigenvalues of A becomes $\lambda_{\max}\le 0$, so that all the eigenvalues of A are nonpositive. While it is clear that the most relevant part of the eigenvalue density lies near the origin, since it determines the behavior of the PSD in the low-frequency limit, it is interesting to notice that the same upper bound and also a lower bound can be found assuming that A is symmetric and using the Gershgorin theorem [14]. In this case the Gershgorin theorem states that every eigenvalue λ satisfies at least one of the inequalities:

$$-\sum_{\substack{j=1,n\\ j\neq k}}a_{kj}\le\lambda-\frac{1}{\tau_k}\le\sum_{\substack{j=1,n\\ j\neq k}}a_{kj}, \tag{31}$$

i.e., all the eigenvalues are contained in the range

$$-\frac{2}{\tau_{\min}}\le\lambda\le 0. \tag{32}$$

Now a question arises: when is A singular, i.e., when is 0 its maximum eigenvalue? This is very important for the PSD, since the sum (26) diverges quadratically when $\omega\to 0$ if 0 is an eigenvalue of A. The idealized systems that we have studied so far look promising, insofar as they give PSD's which are superpositions of many simple relaxation spectra, but they admit $\lambda_{\max}=0$ and thus they may have divergent PSD's. However in real-life systems there is usually a noisy input and an output, so that Eqs. (4) should be modified accordingly:

$$dN_k=-\frac{1}{\tau_k}N_k(t)dt+\sum_{\substack{j=1,n\\ j\neq k}}a_{kj}N_j(t)dt$$
$$+\nu_{0,k}dt+\nu_k(t)dt, \tag{33}$$

where $\boldsymbol{\nu}_0=\{\nu_{0,k}\}_{k=1,\ldots,n}$ is a constant vector, which is the average value of the noisy input, and where

$$\frac{1}{\tau_k}\ge\sum_{\substack{j=1,n\\ j\neq k}}a_{jk}. \tag{34}$$

Moreover (34) must be a strict inequality for at least one site, so that there is at least one output site. The requirement of uniform behavior is satisfied by assuming that the transition probabilities to neighboring sites are always the same.

Typically — for a given topology — we can identify an "inside" and a "boundary" for any set of sites. Then the random walkers in the inside can usually jump only to neighboring sites — and the equal sign holds in

(34)—while the random walkers on the boundary can jump out of the system and (34) is a strict inequality. We also assume that any site can be reached from any other site with a finite sequence of jumps, and that the reverse path is also physically possible. Then the matrix A must be irreducible, and because of (34) it is diagonally dominant, therefore it must be invertible and 0 is not an eigenvalue (see theorem 6.2.27 in [14]). Combining this result with the loose bounds from the Perron and the Gershgorin theorem that we found above, we see that all the eigenvalues are negative and that the PSD can no longer diverge. We make once again the assumption that the stochastic processes $\boldsymbol{\nu}$ are Gaussian uncorrelated processes, such that the statistical descriptions (5a) and (5b) are still valid.

The vector form of Eq. (33) is

$$d\boldsymbol{N} = A\boldsymbol{N}dt + \boldsymbol{\nu}_0 dt + \boldsymbol{\nu}dt, \tag{35}$$

while the corresponding equation for the average values is

$$d\langle \boldsymbol{N}\rangle = A\langle \boldsymbol{N}\rangle dt + \boldsymbol{\nu}_0 dt, \tag{36}$$

and subtracting Eq. (36) from (35) we get

$$d\left(\boldsymbol{N} - \langle \boldsymbol{N}\rangle\right) = A\left(\boldsymbol{N} - \langle \boldsymbol{N}\rangle\right) dt + \boldsymbol{\nu}dt, \tag{37}$$

therefore the spectral results derived in the previous section apply unchanged to the variates $N_k - \langle N_k\rangle$. Notice that Eq. (36) can easily be solved and it is well known that the general solution is [15]

$$\langle N_k\rangle = \{Te^{Dt}T^{-1}\boldsymbol{N}_0\}_k + \langle N_k\rangle_{\text{eq}}, \tag{38}$$

$$= \sum_{j=1}^{n} w_{kj}e^{\lambda_j t} + \langle N_k\rangle_{\text{eq}}, \tag{39}$$

where $\boldsymbol{N}_0$ is the vector of initial values, $\langle N_k\rangle_{\text{eq}}$ are the equilibrium values

$$\langle N_k\rangle_{\text{eq}} = -\left(A^{-1}\boldsymbol{\nu}_0\right)_k, \tag{40}$$

$D = \text{diag}(\lambda_1, \ldots, \lambda_n)$, and T is a matrix whose columns are the eigenvectors of A. Equation (40) is useful in setting up numerical simulations of these processes.

V. THE EIGENVALUE DENSITIES FOR SOME DIFFUSION AND TRANSPORT OPERATORS

We turn now to a detailed analysis of the eigenvalue densities of some linear operators. We take first the case of diffusion along a linear chain of n sites with hopping to nearest neighbors only (the process described at the end of Sec. II), which is associated to the $n \times n$ matrix:

$$A = \begin{pmatrix} -\frac{1}{\tau} & \frac{1}{2\tau} & 0 & 0 & 0 & \cdots \\ \frac{1}{2\tau} & -\frac{1}{\tau} & \frac{1}{2\tau} & 0 & 0 & \cdots \\ 0 & \frac{1}{2\tau} & -\frac{1}{\tau} & \frac{1}{2\tau} & 0 & \cdots \\ 0 & 0 & \frac{1}{2\tau} & -\frac{1}{\tau} & \frac{1}{2\tau} & \cdots \\ \vdots & \vdots & \vdots & \vdots & \vdots & \ddots \end{pmatrix}. \tag{41}$$

Using elementary methods it is easy to show that the eigenvalues of this (symmetric) matrix are

$$\lambda_m = -\frac{1}{\tau}\left(1 - \cos\frac{\pi m}{n+1}\right) \qquad (m = 1, \ldots, n). \tag{42}$$

Therefore the corresponding density for $n \gg 1$ is

$$f_A(\lambda) \approx \frac{1}{n}\left(\frac{dm}{d\lambda_m}\right) \approx \frac{1}{\pi}\frac{1}{\sqrt{|\lambda|(\frac{2}{\tau} - |\lambda|)}}$$

$$\left(-\frac{2}{\tau} + \frac{\pi^2}{2\tau n^2} < \lambda < -\frac{\pi^2}{2\tau n^2}\right), \tag{43}$$

which is dominated by the two large peaks near 0 and near $-\frac{2}{\tau}$. The PSD can be computed directly from (26) and the result is

$$S(\omega) \approx \frac{\sigma^2}{2\pi n}\sum_{m=1}^{n}\frac{1}{\omega^2 + \lambda^2}$$

$$\approx \frac{\sigma^2\tau^2}{2\pi}\int_{1/n}^{1-1/n}\frac{dx}{\omega^2\tau^2 + (1 - \cos\pi x)^2}. \tag{44}$$

From the integral expression (44), it is clear that if $\omega\tau \gg 1$ then $S(\omega) \propto 1/\omega^2$, and if $\omega\tau \ll 1/n^2$ then $S(\omega)$ is approximately constant. In the intermediate region $1 \gg \omega\tau \gg 1/n^2$ the PSD follows approximately the power law $1/f^{1.5}$ as shown in Fig. 1, where the PSD (44) is plotted for different values of n. The complete integrated form of (44) is quite lengthy, and it is difficult to use it to extract the $1/f^{1.5}$ power law. However, a derivation of the $1/f^{1.5}$ power law for $n \gg 1$ is given in Appendix B.

Thus simple 1D diffusion yields a flicker noise, and if n is sufficiently large the effect spans many orders of magnitude. Figure 1 shows that for $n = 500$ the $1/f^{1.5}$ region spans almost four decades, and for large n the $1/f^{1.5}$ region spans approximately $\log_{10}|\frac{\lambda_{\min}}{\lambda_{\max}}| \approx 2\log_{10} n$ decades. The PSD is well-behaved, and the correlation function computed from the Wiener-Kintchine theorem is free of divergences both at low and at high frequency.

The key features of this 1D diffusion model are shared by all the relaxation operators introduced in Sec. IV. We have shown that all the eigenvalues are contained in a range $\lambda_{\min} \le \lambda \le \lambda_{\max} < 0$, and therefore the PSD always approaches the (finite) value $\frac{1}{n}\sum_{k=1}^{n}\frac{1}{\lambda_k^2}$ as ω approaches 0. At the same time the derivative also approaches 0, therefore every PSD flattens to a constant value near the origin. Moreover the eigenvalue range is bounded, therefore for ω large enough, the PSD has a $1/f^2$ behavior, and there must be an intermediate region that interpolates between these behaviors. We have just seen that it may span several orders of magnitude, and it is on this intermediate region that we shall focus our attention from now on. Another important feature shared by these processes is that they are all Gaussian, because they are linear and the driving noise sources are stationary and Gaussian. Furthermore the deterministic part of each process has a simple attractor (since the eigenvalues of A are all negative), therefore the process has a finite

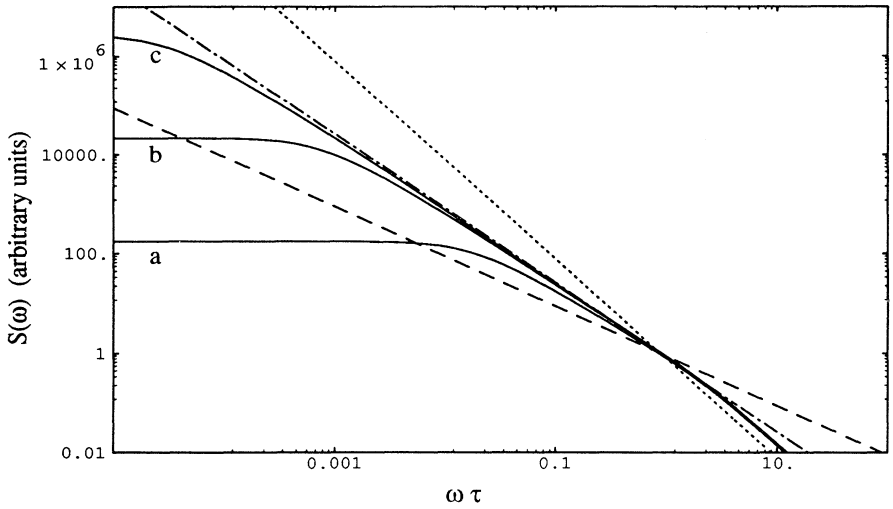

FIG. 1. PSD's for 1D chains of different lengths n calculated using (27). The solid lines show the PSD's for chains with (a) $n = 20$, (b) $n = 100$, and (c) $n = 500$. The straight lines are for reference and represent $1/f^{\alpha}$ spectra with $\alpha = 1$ (dashed), $\alpha = 1.5$ (dashed-dotted), and $\alpha = 2$ (dotted).

variance [16], and it is stationary. This agrees well with past experimental observations of the statistical properties of $1/f$ noise (see the references in the reviews [5–7]). As an independent check of the analytical calculations, I have set up a Monte Carlo program to simulate a 1D chain. At each time step the program loops over all sites, and at each site the populations are updated in parallel according to

$$\Delta N_k \leftarrow \sum_{j=1}^{n} a_{kj} N_j \Delta t + \nu_{0,k} \Delta t + \sigma_k R_k, \tag{45a}$$

$$N_k \leftarrow N_k + \Delta N_k, \tag{45b}$$

where the R_k's are Gaussian pseudorandom numbers with zero mean and unit standard deviation, and the actual standard deviation σ_k of each ΔN_k is computed from the formula

$$\sigma_k^2 = \sum_{j=1}^{n} |a_{kj} \langle N_j \rangle \Delta t| + |\nu_{0,k} \Delta t|. \tag{46}$$

The Gaussian pseudorandom numbers have been generated with the routine **gasdev** described in [17], and modified to use the uniform pseudorandom number generator **ran2** instead of the faster but less safe **ran1** (they are both in the program library [17]).

The simulation included an external noise source at each end of the chain, and the sites have been initialized with the resulting equilibrium values (40). Figure 2 shows a small part of the simulated signal, while Fig. 3 shows the PSD of the simulated process, which provides a nice confirmation of the theoretical result.

In Sec. II, I mentioned that the actual noise statistics cannot be Gaussian, but I concluded that there should be no visible consequence of non-Gaussianity for $aN\Delta t \gg 1$. In order to check this conclusion I have run the simulation program for the 1D chain with "truncated" Gaussian noise, i.e., with noise such that $-\Delta N_k(t) < N_k(t)$ for all k's. In this case the relevant parameter is the average population change $2aN\Delta t \approx (1/\tau)\langle N \rangle \Delta t$. I went down to $(1/\tau)\langle N \rangle \Delta t = 1$ without detecting any deviation from the PSD obtained with pure Gaussian noise.

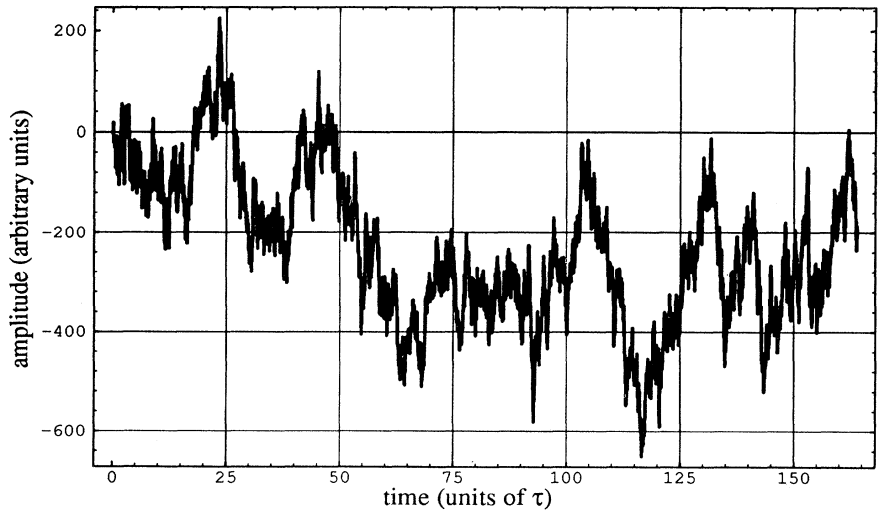

FIG. 2. A small portion (4096 samples) of the simulated signal for a 1D chain with 100 sites and with a noise source at each end of the chain. The signal is the population fluctuation of the middle element (site 50). The relaxation time is $\tau = 0.5$ and the simulation step is $\Delta t = 0.02$ (arbitrary time units).

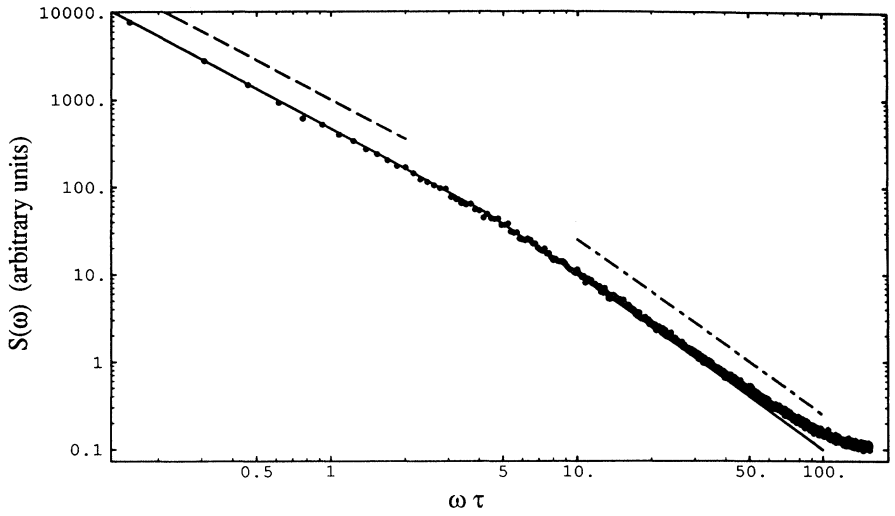

FIG. 3. PSD of the population fluctuations of the middle site (site 50) of a 1D chain of 100 sites and with a noise source at each end of the chain. 2^{20} samples have been generated and each point is the average of 256 PSD estimates obtained from records of 2048 samples each. The relaxation time is $\tau = 0.5$ and the simulation step is $\Delta t = 0.02$ (arbitrary time units). The solid curve is the theoretical curve (b), shown in Fig. 1. The dashed line shows the slope of a $1/f^{1.5}$ spectrum, while the dashed-dotted line shows the slope of a $1/f^2$ spectrum. The departure from the $1/f^2$ behavior at high frequency is due both to the comparatively large time step and to aliasing.

We change now the lattice connectivity either by allowing jumps to more distant sites, or stepping up in the number of dimensions. Let us start with a 1D diffusion process with a probability of jumping from site j to site k that decreases quadratically with the distance $|j-k|$, i.e., we take matrix elements $a_{jk} = \frac{\kappa}{|j-k|^2}$, $a_{kk} = -\frac{1}{\tau} = -\max_k \left\{\sum_{j\neq k} a_{jk}\right\}$. The associated relaxation matrix is

$$A = \begin{pmatrix} -\frac{1}{\tau} & \kappa & \frac{\kappa}{4} & \frac{\kappa}{9} & \frac{\kappa}{16} & \cdots \\ \kappa & -\frac{1}{\tau} & \kappa & \frac{\kappa}{4} & \frac{\kappa}{9} & \cdots \\ \frac{\kappa}{4} & \kappa & -\frac{1}{\tau} & \kappa & \frac{\kappa}{4} & \cdots \\ \frac{\kappa}{9} & \frac{\kappa}{4} & \kappa & -\frac{1}{\tau} & \kappa & \cdots \\ \vdots & \vdots & \vdots & \vdots & \vdots & \ddots \end{pmatrix}, \tag{47}$$

with $\frac{1}{\tau} \approx 2\kappa \sum_{n=0}^{\infty} \frac{1}{n^2} = \frac{\kappa\pi^2}{3}$. We can still find the eigen-

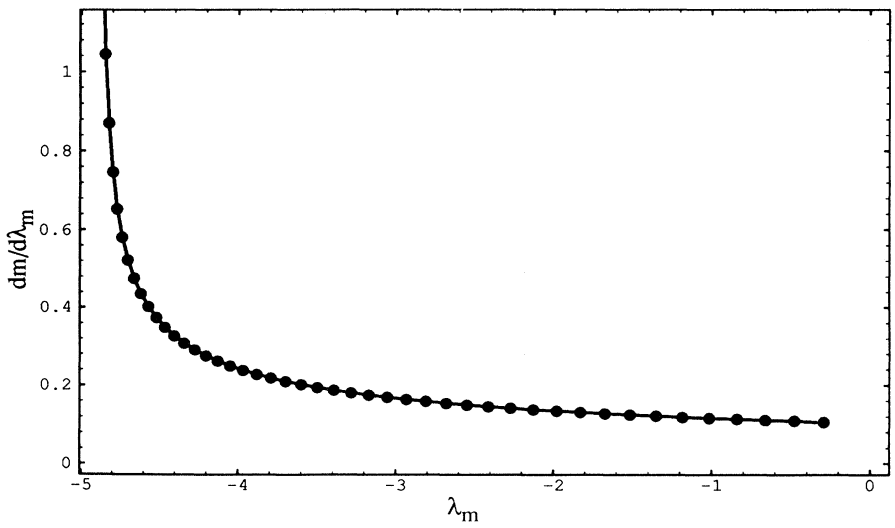

FIG. 4. Eigenvalue density for the 1D chain with matrix elements $a_{jk} = 1/|j-k|^2$ if $j \neq k$, $a_{kk} = -1/\tau = \pi^2/3$, and $n = 50$. The dots show the numerical result (obtained with the Jacobi algorithm, see [14,17]), while the dotted line shows the approximate theoretical curve.

values of this matrix by elementary methods, and they are

$$\tau\lambda_m = -3\left(\frac{m}{n+1} - \frac{m^2}{2(n+1)^2}\right) \qquad (m = 1, \ldots, n). \tag{48}$$

This expression is exact for $n \to \infty$, however it gives a fairly good approximation of the eigenvalues of matrices like (47) even when their dimension is not too large: Fig. 4 shows that the eigenvalue density obtained from the eigenvalues computed with the numerical Jacobi method [17] for $n = 50$ is practically indistinguishable — at the scale of the plot — from the density derived from (48). The eigenvalue density in Fig. 4 is nearly flat in a large region near the origin, therefore we expect to find a large $1/f$ region in the PSD. Indeed, using (26) and the eigenvalues obtained numerically, we obtain the curve shown in Fig. 5 for $n = 50$ and $\kappa = 1$, where an extended $1/f$ region is clearly visible. This nice $1/f$ behavior is the exception rather than the rule for one-dimensional systems, which seem to be more prone to follow the behavior displayed by the nearest neighbor interactions described at the beginning of this section (see Figs. 6 and 7).

We consider now two- and three-dimensional lattices with hopping to nearest neighbors only. Take, e.g., a 3×3, 2D lattice with the sites labeled

$$\begin{array}{ccc} 1 & 2 & 3 \\ 4 & 5 & 6 \\ 7 & 8 & 9 \end{array}$$

so that the associated matrix is

$$A = \begin{pmatrix} -\frac{1}{\tau} & \frac{1}{4\tau} & 0 & \frac{1}{4\tau} & 0 & 0 & 0 & 0 & 0 \\ \frac{1}{4\tau} & -\frac{1}{\tau} & \frac{1}{4\tau} & 0 & \frac{1}{4\tau} & 0 & 0 & 0 & 0 \\ 0 & \frac{1}{4\tau} & -\frac{1}{\tau} & \frac{1}{4\tau} & 0 & \frac{1}{4\tau} & 0 & 0 & 0 \\ \frac{1}{4\tau} & 0 & \frac{1}{4\tau} & -\frac{1}{\tau} & \frac{1}{4\tau} & 0 & \frac{1}{4\tau} & 0 & 0 \\ 0 & \frac{1}{4\tau} & 0 & \frac{1}{4\tau} & -\frac{1}{\tau} & \frac{1}{4\tau} & 0 & \frac{1}{4\tau} & 0 \\ 0 & 0 & \frac{1}{4\tau} & 0 & \frac{1}{4\tau} & -\frac{1}{\tau} & \frac{1}{4\tau} & 0 & \frac{1}{4\tau} \\ 0 & 0 & 0 & \frac{1}{4\tau} & 0 & \frac{1}{4\tau} & -\frac{1}{\tau} & \frac{1}{4\tau} & 0 \\ 0 & 0 & 0 & 0 & \frac{1}{4\tau} & 0 & \frac{1}{4\tau} & -\frac{1}{\tau} & \frac{1}{4\tau} \\ 0 & 0 & 0 & 0 & 0 & \frac{1}{4\tau} & 0 & \frac{1}{4\tau} & -\frac{1}{\tau} \end{pmatrix}, \tag{49}$$

such that the probability of jumping to any given neighboring site is always the same, the relaxation time is also the same for all sites, and the random walkers can leave the lattice from all the $(2n_x + 2n_y - 4)$ sites on the boundary. Once again it is easy to show that for a rectangular lattice of $n_x \times n_y$ sites the eigenvalues are

$$\lambda_{jk} = -\frac{1}{2\tau}\left(2 - \cos\frac{\pi j}{n_x + 1} - \cos\frac{\pi k}{n_y + 1}\right)$$

$$(j = 1, \ldots, n_x; \quad k = 1, \ldots, n_y). \tag{50}$$

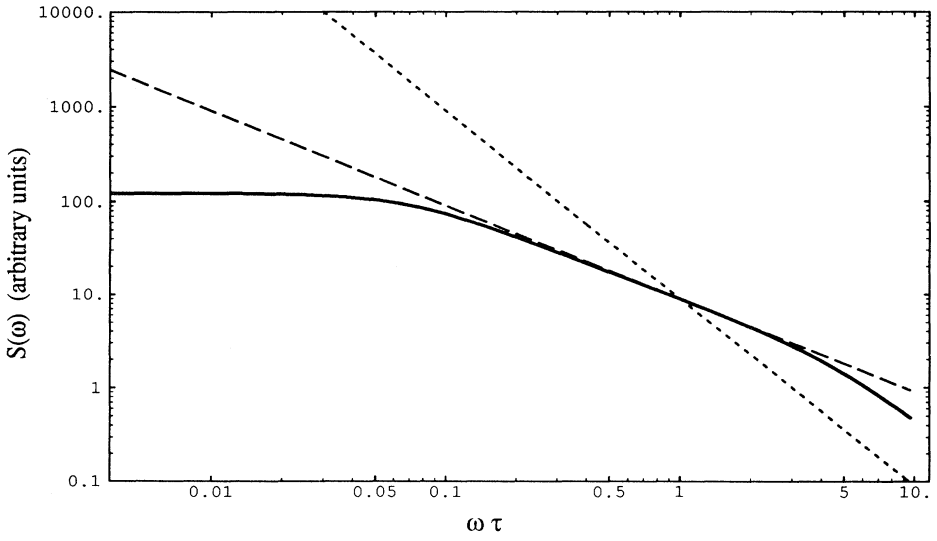

FIG. 5. PSD obtained analytically from the eigenvalue density of Fig. 4 and from (27). The straight lines are for reference and represent $1/f^\alpha$ spectra with $\alpha = 1$ (dashed) and $\alpha = 2$ (dotted).

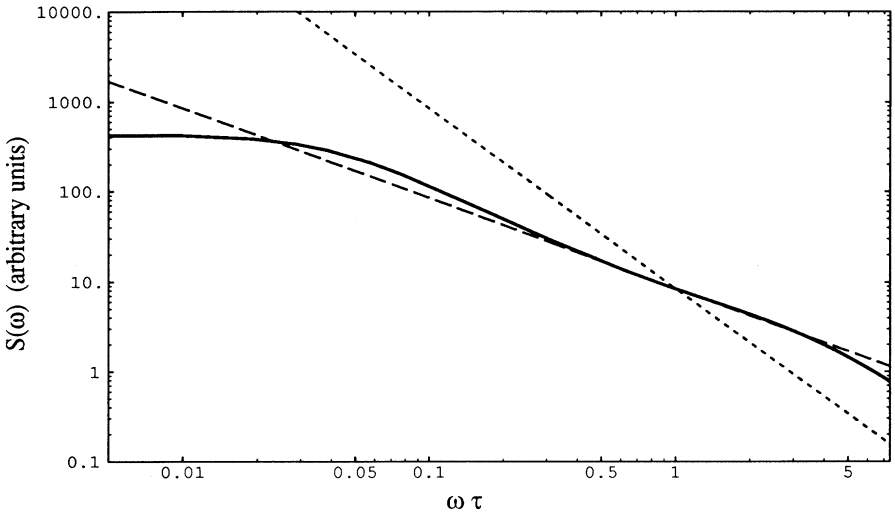

FIG. 6. PSD for the 1D chain with long range $\kappa^{-|j-k|}$ couplings (here $\kappa = 0.6$, $n = 50$). The straight lines are for reference and represent $1/f^{\alpha}$ spectra with $\alpha = 1$ (dashed) and $\alpha = 2$ (dotted).

Similarly for a 3D lattice of $n_x \times n_y \times n_z$ sites the eigenvalues are

$$\lambda_{jkl} = -\frac{1}{3\tau}\left(3 - \cos\frac{\pi j}{n_x+1} - \cos\frac{\pi k}{n_y+1} - \cos\frac{\pi l}{n_z+1}\right)$$

$$(j = 1,\ldots,n_x; \quad k = 1,\ldots,n_y; \quad l = 1,\ldots,n_z). \quad (51)$$

These expressions are very similar to (42), but yield substantially different eigenvalue densities. As it is shown in Appendix B, the 2D square lattice leads to an eigenvalue density which is very nearly flat near the origin, and therefore the resulting PSD has a $1/f$ shape, while the PSD for the 3D cubic lattice has a $1/f^{0.5}$ shape, and thus models with nearest neighbor interactions yield different behaviors for different lattice dimensions. It is also clear that as one of the sides of, e.g., the 3D lattice is reduced, the eigenvalue density changes and approaches the eigenvalue density of the 2D lattice (the new density, though, is only proportional to, and not equal to, the density for the 2D lattice, because the limiting form of the 3D lattice allows the random walkers to jump out of the lattice at each lattice site, and not just along the sides of the 2D lattice). Therefore lattices with arbitrary sides interpolate between the 1D, 2D, and 3D lattices.

Before concluding this Sec. I wish to discuss the role of transport in a model with nearest neighbor interactions, as it was introduced at the end of Sec. II. It is easy to show that instead of (42) we have

$$\lambda_m = -\frac{1}{\tau}\left(1 - \sqrt{4pq}\cos\frac{\pi m}{n+1}\right) \qquad (m = 1,\ldots,n). \quad (52)$$

The product $4pq$ attains its maximum value 1 when $p = q = 1/2$ and decreases whenever there is drift, therefore transport has the effect of "compressing" the whole eigenvalue distribution about its middle value $1/\tau$, and

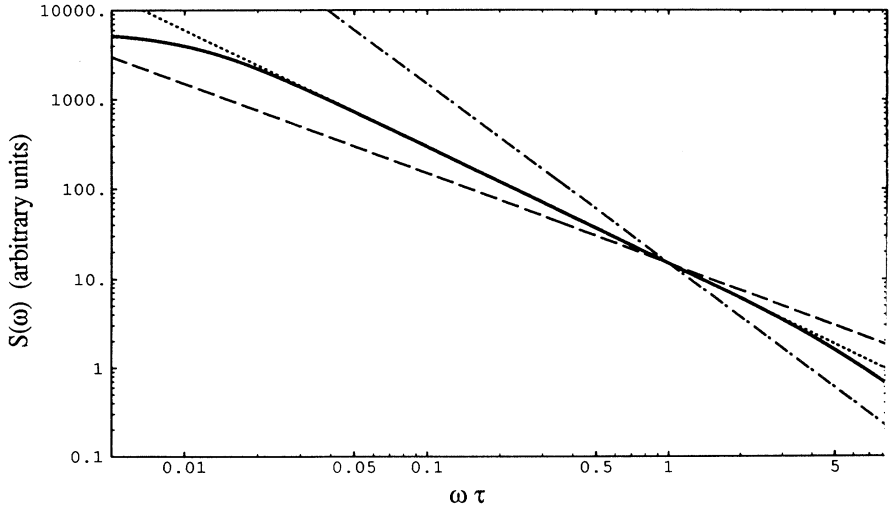

FIG. 7. PSD for the 1D chain with long range $1/|j-k|^3$ couplings (here $n = 50$). The straight lines are for reference and represent $1/f^{\alpha}$ spectra with $\alpha = 1$ (dashed), $\alpha = 1.3$ (dotted), and $\alpha = 2$ (dashed-dotted).

as either p or q increases the PSD changes more and more to the simple $1/(\omega^2+\lambda^2)$ shape. It seems that transport does more harm than good and takes us away from a $1/f$ shape, however the physical systems that are known to display $1/f$ noise usually are *not* one dimensional. So it makes sense to consider again the 2D and 3D lattices introduced above, and after some straightforward but tedious calculations one finds that the eigenvalues are

$$\lambda_{jk}=-\frac{1}{2\tau}\left[2-\cos\frac{\pi j}{n_x+1}-\sqrt{4pq}\cos\frac{\pi k}{n_y+1}\right]$$
$$(j=1,\ldots,n_x;\quad k=1,\ldots,n_y) \quad (53)$$

for the 2D lattice with transport along y, and

$$\lambda_{jkl}=-\frac{1}{3\tau}\left[3-\cos\frac{\pi j}{n_x+1}-\cos\frac{\pi k}{n_y+1}-\sqrt{4pq}\cos\frac{\pi l}{n_z+1}\right]$$
$$(j=1,\ldots,n_x;\quad k=1,\ldots,n_y;\quad l=1,\ldots,n_z) \quad (54)$$

for the 3D lattice with transport along z, so that in these cases the PSD should have a $1/f^\alpha$ shape with α between 1 and 1.5 for the 2D lattice and between 0.5 and 1 for the 3D lattice.

VI. CONDUCTANCE FLUCTUATIONS

If we aim at explaining $1/f$ noise in resistors, then the overall picture is satisfactory but still incomplete, because the lattices described above do not really represent reasonable transport channels. Now I define a 3D transport channel as a simple cubic lattice of $n=n_x\times n_y\times n_z$ sites (so that each site is labeled by three indices i,j,k), with drift along the z direction, and with two "interfaces" at $k=1$ and $k=n_z$ (1D and 2D channels, i.e., "wires" and "strips" are obtained by setting $n_x=n_y=1$ and $n_y=1$, respectively). Charge is exchanged only at these interfaces, and here the transport channel may both lose and gain charge. With the labeling defined above, the matrix elements of A for a 3D transport channel are

$$\begin{aligned}
a_{ijk;ijk}&=-1/\tau;\quad (1<i<n_x, 1<j<n_y)\\
a_{1jk;1jk}&=a_{n_xjk;n_xjk}=-5/6\tau;\quad (1<j<n_y)\\
a_{i1k;i1k}&=a_{in_yk;in_yk}=-5/6\tau;\quad (1<i<n_x)\\
a_{11k;11k}&=a_{1n_yk;1n_yk}=a_{n_x1k;n_x1k}\\
&=a_{n_xn_yk;n_xn_yk}=-4/6\tau;\\
a_{ij,k+1;ijk}&=p/3\tau;\quad a_{ij,k-1;ijk}=q/3\tau;\\
a_{i\pm1,jk;ijk}&=a_{i,j\pm1,k;ijk}=1/6\tau;\\
a_{ijk,rst}&=0;\quad \text{(all remaining matrix elements)},
\end{aligned} \quad (55)$$

where p and q have the same meaning as in Sec. II. These matrix elements mean that the transition rates to neighbors are the same for every site of the lattice, and that the relaxation times are also the same for all sites in the bulk and on the interfaces, while they change slightly for sites on the boundary (the matrix elements for the 2D channel are very similar). The eigenvalues corresponding to these matrices are

$$\lambda_{jk}=-\frac{1}{2\tau}\left[2-\cos\frac{\pi j}{n_x}-\sqrt{4pq}\cos\frac{\pi k}{n_y+1}\right]$$
$$(j=0,\ldots,n_x-1;\quad k=1,\ldots,n_y) \quad (56)$$

for the 2D transport channel with transport along y, and

$$\lambda_{jkl}=-\frac{1}{3\tau}\left[3-\cos\frac{\pi j}{n_x}-\cos\frac{\pi k}{n_y}-\sqrt{4pq}\cos\frac{\pi l}{n_z+1}\right]$$
$$(j=0,\ldots,n_x-1;\quad k=0,\ldots,n_y-1;\quad l=1,\ldots,n_z) \quad (57)$$

for the 3D transport channel with transport along z.

Notice that if d is the lattice dimension, δ is the lattice spacing, $p\approx q\approx 0.5$, and $L=n_z\delta$ is the channel length, the smallest eigenfrequency is $|\lambda_{\max}|\approx\frac{\pi^2}{2dn_z^2\tau}$, and since $\tau=\frac{\delta^2}{D}$, then $|\lambda_{\max}|\approx\frac{\pi^2 D}{2dL^2}$. The diffusion time $|\lambda_{\max}|^{-1}$ is approximately the average lifetime of the longest lived transient in (39), therefore if there is no source, this is also the average time needed to empty the transport channel. However, it is also clear that if the contacts to the "outside" have a cross-section which is smaller than the cross-section of the transport channel, then $|\lambda_{\max}|$ becomes smaller (i.e., it takes longer to empty the channel). Indeed the limiting case of a transport channel with no input-output (and no drift) has eigenvalues

$$\lambda_{jkl}=-\frac{1}{3\tau}\left[3-\cos\frac{\pi j}{n_x}-\cos\frac{\pi k}{n_y}-\cos\frac{\pi l}{n_z}\right]$$
$$(j=0,\ldots,n_x-1;\quad k=0,\ldots,n_y-1;$$
$$l=0,\ldots,n_z-1) \quad (58)$$

and $|\lambda_{\max}|=0$. This is something that we already knew from Sec. IV, however Eqs. (57) and (58) show that the eigenvalues do not change appreciably when one shuts down the channel, while the diffusion time $|\lambda_{\max}|^{-1}$ becomes much larger than the previously estimated $\frac{\pi^2 D}{2dL^2}$, thereby increasing the range of the $1/f^\alpha$ region.

The PSD's can be computed from (56) and (57) and they have the same general behavior as the 2D and 3D lattices discussed in the previous section: examples are shown in Figs. 8 and 9. Figure 10 shows a simulated signal for the 2D channel.

I assume a noisy source of charge at each end of the transport channel, and for given noise rates, it is easy to compute the equilibrium values $\langle N_{ijk}\rangle_{\rm eq}$: if the noise source at the "entrance" of the transport channel has an average rate $p\nu_0$ and the noise source at the "exit" has an average rate $q\nu_0$, then all the sites have the same equilibrium population $\langle N\rangle_{\rm eq}=\langle N_{ijk}\rangle_{\rm eq}=\tau\nu_0$, and the environment is uniform (Fig. 11 illustrates this point for a

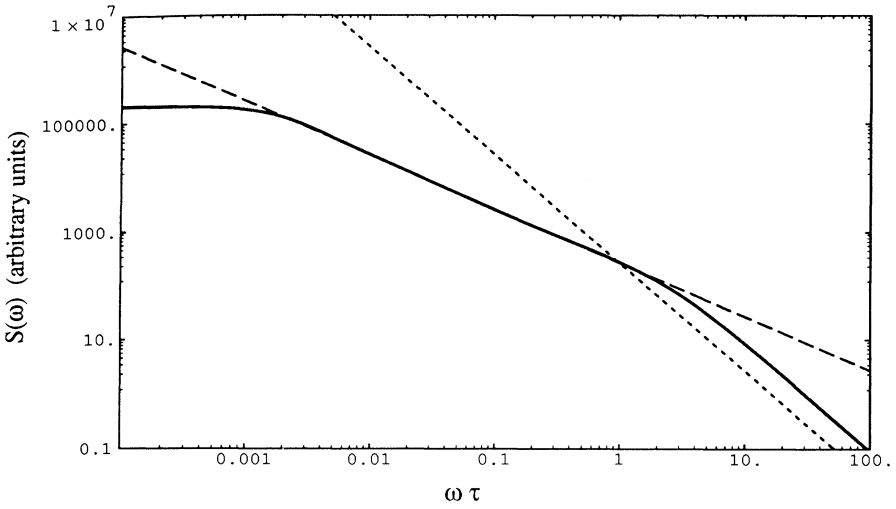

FIG. 8. PSD for the 2D transport channel ($n_x = 20$, $n_z = 45$). The straight lines are for reference and represent $1/f^\alpha$ spectra with $\alpha = 1$ (dashed) and $\alpha = 2$ (dotted).

1D chain). This is especially important if the model is to represent a resistor, because it means that on the average the charge density is the same over the whole transport channel, i.e., there are no (averaged) space charge effects. At the same time this requirement satisfies the uniformity hypothesis that was used to find the PSD.

A simple approximation of the current PSD can now be obtained as follows. The net flow of charge carriers across any section of the transport channel (number of carriers per unit time) is given by

$$\text{flow across } k\text{th section} \approx (\text{particles that move to +ve } z) - (\text{particles that move to -ve } z)$$
$$\approx \sum_{\substack{i=1,n_x \\ j=1,n_y}} \left(\frac{p}{\tau} N_{i,j,k} - \frac{q}{\tau} N_{i,j,k}\right) = \frac{(p-q)}{\tau} \sum_{\substack{i=1,n_x \\ j=1,n_y}} N_{i,j,k} \tag{59}$$

and therefore the average electric current is

$$\langle I \rangle \approx \frac{Aev}{\delta^3} \langle N \rangle_{\text{eq}}, \tag{60}$$

where δ is the lattice spacing, $v = (p-q)\frac{\delta}{\tau}$ is the drift speed, $A = n_x n_y \delta^2$ is the cross-section of the transport channel, and e is the charge of each carrier. Now let S_I be the PSD of the electric current I. Then

$$S_I(\omega) \approx \frac{(p-q)^2 e^2}{\tau^2} \lim_{T\to\infty} \frac{1}{2\pi T} \left\langle \left| \sum_{\substack{i=1,n_x \\ j=1,n_y}} F_{ijk}(\omega) \right|^2 \right\rangle, \tag{61}$$

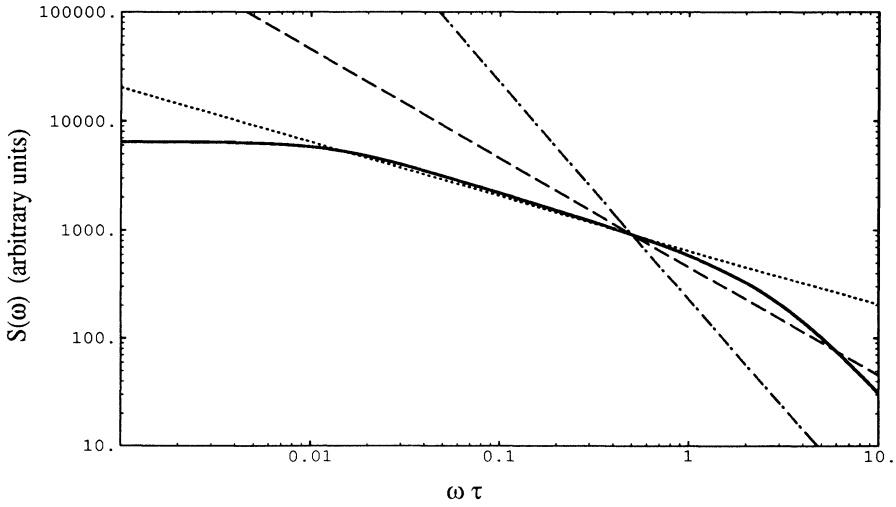

FIG. 9. PSD for the 3D transport channel ($n_x = 15$, $n_y = 15, n_z = 15$). The straight lines are for reference and represent $1/f^\alpha$ spectra with $\alpha = 1$ (dashed), $\alpha = 0.5$ (dotted), and $\alpha = 2$ (dashed-dotted).

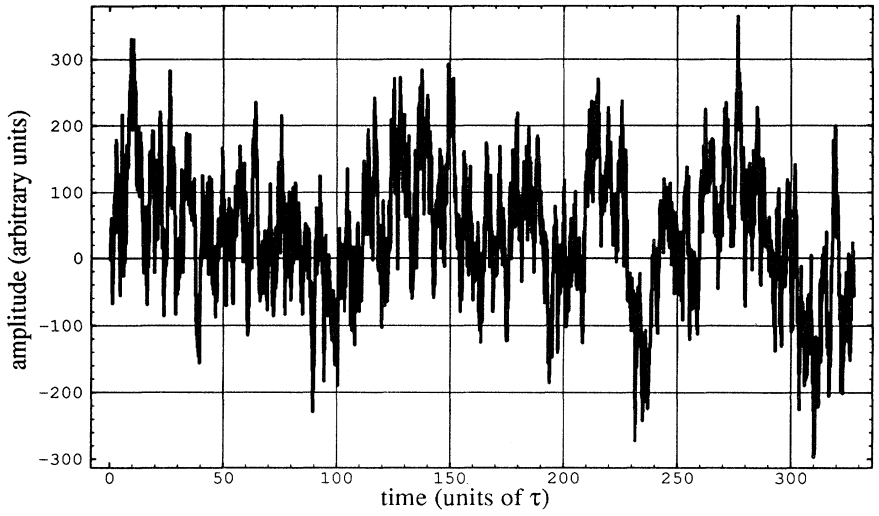

FIG. 10. A small portion (4096 samples) of the simulated signal for a 2D transport channel ($n_x = 20, n_z = 45$) with a noise source at each end of the channel (the signal is the population fluctuation at the center of the channel). The relaxation time is $\tau = 0.25$ and the simulation step is $\Delta t = 0.02$ (arbitrary time units).

$$= \frac{(p-q)^2 e^2}{\tau^2} \lim_{T\to\infty} \frac{1}{2\pi T} \times \sum_{\substack{i=1,n_x \\ j=1,n_y}} \sum_{\substack{l=1,n_x \\ m=1,n_y}} \langle F^*_{ijk}(\omega) F_{lmk}(\omega)\rangle, \tag{62}$$

$$= \left(\frac{Aev\rho}{\delta^3}\right)^2 S(\omega), \tag{63}$$

$$\approx \rho^2 \frac{\langle I\rangle^2}{\langle N\rangle^2_{\rm eq}} \frac{\sigma^2}{2\pi} \int_{|\lambda_{\rm min}|}^{|\lambda_{\rm max}|} \frac{f_A(|\lambda|)}{\omega^2 + |\lambda|^2} d|\lambda|, \tag{64}$$

$$\approx \frac{\rho^2 \langle I\rangle^2}{2\pi\tau \langle N\rangle_{\rm eq}} \int_{|\lambda_{\rm min}|}^{|\lambda_{\rm max}|} \frac{f_A(|\lambda|)}{\omega^2 + |\lambda|^2} d|\lambda|, \tag{65}$$

where $\sigma^2 \approx 2\langle N\rangle_{\rm eq}/\tau$ has been used. The cross-correlation terms that appear in (62) have the same frequency dependence as the PSD (see Appendix C), and ρ is a lattice-specific constant. The coefficient ρ can be computed (see Appendix C), but here we do not need to carry out this calculation, as we shall shortly see.

Notice that the integral in (65) approaches the value $\frac{1}{n}\sum_{k=1}^{n} \frac{1}{|\lambda_k|^2}$ as $\omega \approx |\lambda_{\rm max}|$, and if $n \gg 1$, $|\lambda_{\rm max}|$ is very small and $\frac{1}{n}\sum_{k=1}^{n} \frac{1}{|\lambda_k|^2} \approx \frac{1}{n} \frac{1}{|\lambda_{\rm max}|^2}$. Therefore, in the range $|\lambda_{\rm min}| < \omega < |\lambda_{\rm max}|$, the integral in (65) is approximately equal to $\frac{1}{n|\lambda_{\rm max}|^2} \left(\frac{|\lambda_{\rm max}|}{\omega}\right)^{\alpha}$, and then

$$\frac{S_I(\omega)}{\langle I\rangle^2} \approx \frac{\rho^2}{2\pi\tau n \langle N\rangle_{\rm eq} |\lambda_{\rm max}|^2} \left(\frac{|\lambda_{\rm max}|}{\omega}\right)^{\alpha} = \left(\frac{\rho^2}{2\pi\tau |\lambda_{\rm max}|^2}\right) \frac{1}{N_{\rm tot}} \left(\frac{|\lambda_{\rm max}|}{\omega}\right)^{\alpha}, \tag{66}$$

where $N_{\rm tot} = n\langle N\rangle_{\rm eq}$ is the total number of charge carriers in the channel. Now remember that if G is the conductance then $S_I(\omega)/\langle I\rangle^2 = S_G(\omega)/\langle G\rangle^2$ and therefore Eq. (66) gives the PSD of conductance fluctuations as well, and corresponds to the Hooge formula [18]. In view of the previous discussion on $\lambda_{\rm max}$, it is clear that the coefficient in front of the $N_{\rm tot}^{-1}\omega^{-\alpha}$ dependence has no fundamental significance (and therefore it is useless to compute ρ).

VII. CONCLUSIONS

I have described a mathematical mechanism whereby flicker noise appears as a natural feature of a collection of identical interacting relaxing systems driven by white noise. In the Introduction I have already mentioned the diffusion model of Voss and Clark [9]. Similar studies — to cite just a few — are those of Liu, Jensen, and Grinstein, Hwa, and Jensen [19]. However, the authors of these papers obtain only rough approximations of the Green's functions of the linear diffusion problems, while

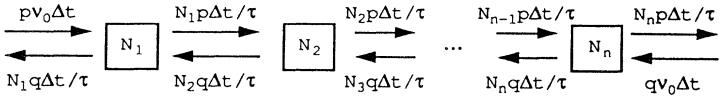

FIG. 11. Schematic representation of the average population exchanges between sites of a 1D chain during a time interval of duration Δt. When the external sources have the average rates shown in the figure, every site has the same average equilibrium population, i.e., $\langle N_1\rangle = \langle N_2\rangle = \cdots = \langle N_n\rangle = \nu_0\tau$.

here I have carried out a mathematical procedure that amounts to an exact calculation of the Green's function, and I have explicitly displayed the properties of some lattices with both diffusion and transport. I wish also to stress the importance of having $1/f$ noise from linear processes: this agrees well with most experimental observations of $1/f$ noise statistics, and entails a considerable mathematical simplification. This is not to say that nonlinear approaches such as [20] are to be discounted, but it is certainly harder to fit the observed Gaussianity to these processes and it is also harder to identify the relevant macroscopic parameters (see the discussion on nonlinear Langevin equations in [21]). Other features of the mechanism studied in this paper are as follows:

All the eigenvalues are negative and lie in a finite range as a consequence of boundary effects and finite system size, and therefore the PSD is quite regular and there are no disturbing infinite quantities: this is quite reassuring in view of the paradoxical consequences of "true" $1/f$ noise discussed in [22].

Generic PSD's for diffusion processes should be of the form $1/f^{\alpha}$ with $0.5 < \alpha < 1.5$ and $\alpha = 1$ has no special significance, apart from the fact that nearly all the observed systems are approximately two-dimensional, and $\alpha = 1$ is exactly what one should expect from the simple diffusion model for a 2D system (indeed experiments observe a whole range of values of α in the vicinity of 1; see the list of α values in [5]).

Given the probabilistic nature of the interaction between different sites, noise is self-generated by the system, and there is no real need for an external noise source.

The thermal diffusion theory of Voss and Clark [9] was troubled after its appearance by several problems (listed in [18]), and especially by the lack of spatial correlations. Though at the beginning there appeared to be some correlations, they were not found by later experiments (see, e.g., [23]). As in *any* diffusion theory, spatial correlation must be present also in the treatment of this paper. However, none of the experiments that ruled out the Voss and Clark model applies here. This important point is discussed in Appendix C.

The model of a transport channel also explains, at least qualitatively, some other facts like the steepening of the PSD observed at low temperatures by Voss and Clark [9] and by Eberhard and Horn [24]. In fact the difference $(p-q)$ is related to the current flowing in the sample by

$$(p-q) = \frac{I\tau}{A(eN/\delta^3)\delta} \tag{67}$$

(eN/δ^3 is the charge density), therefore, if the current is held fixed while the temperature is lowered, the difference $(p-q)$ increases since the relaxation time τ also increases. Then the factor $\sqrt{4pq} = \sqrt{1-(p-q)^2}$ decreases and the eigenvalues (whatever the dimensionality of the lattice) are compressed about their average value, and the PSD becomes steeper.

I also wish to point out that this mechanism applies whenever there are relaxing linear systems, and diffusion and transport are just special cases. The PSD's obtained for some 1D systems with long-range interactions suggest that it might be an explanation for $1/f$ noise in many systems other than resistors. And indeed I have generated random matrices and have found hints of a "universality" that goes beyond simple transport channels. In one instance I have taken symmetric random matrices $A = \{a_{jk}\}$ such that the off-diagonal elements are almost everywhere zero, apart from two randomly chosen elements in each row (these elements may also coincide). The nonzero off-diagonal elements are themselves random numbers with a uniform density between 0 and 1. Then, row by row, the diagonal elements are the negative of the sum of the off-diagonal elements in each row, minus a number much smaller than 1, so that (34) is a strict inequality. These random matrices have the same average number of nonzero off-diagonal terms as the 1D chain of Sec. II, however they are not granted to be irreducible. Figure 12 shows that "on average" these matrices have the same PSD as the 1D chain.

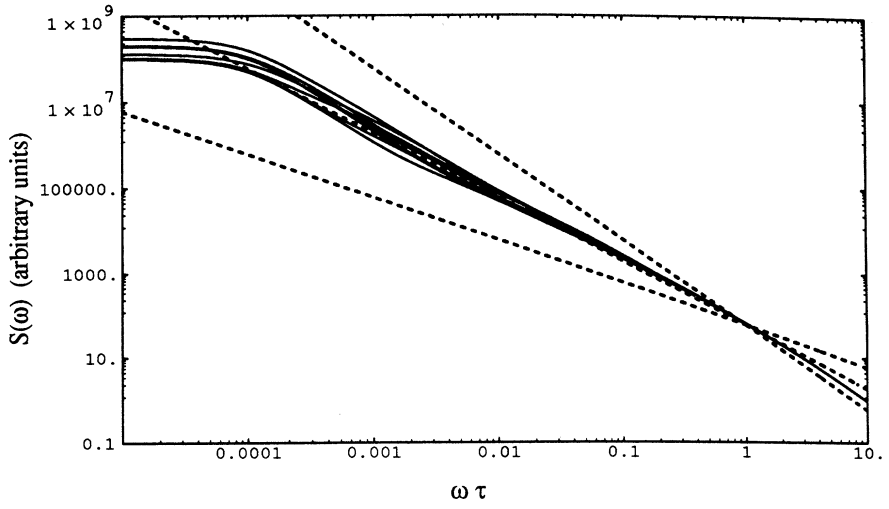

FIG. 12. PSD's for ten random relaxation matrices with approximately two nonzero off-diagonal elements in each row. The matrices have dimension 100 and the eigenvalues have been computed numerically, then the PSD's have been computed using Eq. (26). The dotted straight lines have slopes 1, 1.5, and 2: notice that the computed PSD's closely follow the $1/f^{1.5}$ line over four orders of magnitude.

APPENDIX A

If all the random-walkers see the same average environment we may define an average $\langle|F|^2\rangle$, and use formula (16) to obtain

$$\langle|F|^2\rangle \approx \frac{1}{n}\left\langle\sum_{j=1}^{n}|F_j|^2\right\rangle, \tag{A1}$$

$$= \frac{1}{n}\langle \boldsymbol{F}^\dagger\cdot\boldsymbol{F}\rangle, \tag{A2}$$

$$= \frac{1}{n}\left\langle \boldsymbol{f}^\dagger\left[(i\omega\mathbb{1}-A)^{-1}\right]^\dagger\cdot\left[(i\omega\mathbb{1}-A)^{-1}\right]\boldsymbol{f}\right\rangle, \tag{A3}$$

$$= \frac{1}{n}\left\langle\sum_{j,k,l} f_j^*\left[(i\omega\mathbb{1}-A)^{-1}\right]^\dagger_{jk} \times\left[(i\omega\mathbb{1}-A)^{-1}\right]_{kl} f_l\right\rangle, \tag{A4}$$

$$= \frac{1}{n}\sum_{j,l}\left\{\left[(i\omega\mathbb{1}-A)^{-1}\right]^\dagger\cdot\left[(i\omega\mathbb{1}-A)^{-1}\right]\right\}_{jl} \times\langle f_j^* f_l\rangle. \tag{A5}$$

From the independence of the noise processes and from the assumed uniformity of the average environment:

$$\langle|F|^2\rangle \approx \frac{1}{n}\sum_{j,l}\left\{\left[(i\omega\mathbb{1}-A)^{-1}\right]^\dagger\cdot\left[(i\omega\mathbb{1}-A)^{-1}\right]\right\}_{jl} \times\delta_{jl}\langle|f_l|^2\rangle \tag{A6}$$

$$= \frac{1}{n}\langle|f|^2\rangle\mathrm{Tr}\left\{\left[(i\omega\mathbb{1}-A)^{-1}\right]^\dagger\cdot\left[(i\omega\mathbb{1}-A)^{-1}\right]\right\}. \tag{A7}$$

The relaxation matrices A that we consider in this paper are real matrices. Since they are nonsingular they are certainly diagonalizable, unless there are degenerate eigenvalues such that they can only be put in a Jordan quasidiagonal form. However, in a physical environment the degeneracy is likely to be removed by any small randomness in the matrix elements. This does not affect substantially the shape of the PSD, because the eigenvalue spectrum is stable against small perturbations (see Sec. 6.3 in [14]). Now let $\boldsymbol{\eta}$ be an eigenvector of A, so that $A\boldsymbol{\eta}=\lambda\boldsymbol{\eta}$, then $\boldsymbol{\eta}^+$ is a left eigenvector of A^t with eigenvalue λ^*, i.e., $\boldsymbol{\eta}^+A^t=\lambda^*\boldsymbol{\eta}$ (see [14] for the algebra of left and right eigenvectors). If we take normalized left and right eigenvectors, i.e., $\boldsymbol{\eta}_j^+\boldsymbol{\eta}_k=\delta_{jk}$, Eq. (A7) can also be written as

$$\langle|F|^2\rangle \approx \frac{1}{n}\langle|f|^2\rangle\sum_{j,l}\boldsymbol{\eta}_l^\dagger\left[(i\omega\mathbb{1}-A)^{-1}\right]^\dagger\cdot\left[(i\omega\mathbb{1}-A)^{-1}\right]\boldsymbol{\eta}_l, \tag{A8}$$

$$= \frac{1}{n}\langle|f|^2\rangle\sum_{j=1}^{n}\frac{1}{-i\omega-\lambda_j^*}\frac{1}{i\omega-\lambda_j}, \tag{A9}$$

$$= \frac{1}{n}\langle|f|^2\rangle\sum_{j=1}^{n}\frac{1}{\omega^2+|\lambda_j|^2}, \tag{A10}$$

which is the same as (25) (see also theorem 4.4.3 in [14]). Some information has been lost in this proof. We have not found the individual PSD's for the populations at each site, but rather an average PSD. However, something else has been gained. Now the proof has been extended to incorporate nonsymmetrical matrices; this means that the results of Sec. III hold for the symmetrical case of diffusion as well as for the nonsymmetrical case of transport.

APPENDIX B

Take a set of eigenvalues $\{\lambda_m\}_{m=1,\ldots,n}$ such that $\lambda_m\propto m^2$ for small m, so that for large n, $\lambda(t)\approx\alpha t^2$ and one has to compute the integral

$$\int_{\lambda_{\min}}^{\lambda_{\max}}\frac{dt}{\omega^2+\alpha^2t^4} \tag{B1}$$

to find the PSD. The result of the indefinite integration is

$$\frac{1}{2\sqrt{2|\alpha|}\omega^{3/2}}\left[\arctan\left(1+t\sqrt{\frac{2|\alpha|}{\omega}}\right)-\arctan\left(1-t\sqrt{\frac{2|\alpha|}{\omega}}\right)\right]+\frac{1}{4\sqrt{2|\alpha|}\omega^{3/2}}\ln_{10}\left(\frac{|\alpha|t^2+t\sqrt{2|\alpha|\omega}+\omega}{|\alpha|t^2-t\sqrt{2|\alpha|\omega}+\omega}\right), \tag{B2}$$

and thus for $\lambda_{\min} \ll \omega \ll \lambda_{\max}$

$$\int_{\lambda_{\min}}^{\lambda_{\max}} \frac{dt}{\omega^2 + \alpha^2 t^4} \approx \frac{\pi}{2\sqrt{2|\alpha|}} \frac{1}{\omega^{3/2}}. \tag{B3}$$

In the case of the 1D chain discussed in Sec. V, $\lambda_m = -\frac{1}{\tau}\left(1 - \cos\frac{\pi m}{n+1}\right) \approx -\frac{\pi^2 m^2}{2\tau n^2}$ for $m \ll n$, $n \gg 1$, and indeed integrating the full expression one finds that

$$\int_{\lambda_{\min}}^{\lambda_{\max}} \frac{dt}{\omega^2 + \lambda^2} \propto \frac{1}{\omega^{1.5}} \tag{B4}$$

for $\lambda_{\min} \ll \omega \ll \lambda_{\max}$. Similarly, for the 2D lattice one finds that the eigenvalues (50) can be approximated by the expression $|\lambda_{jk}| \approx \frac{\pi^2 j^2}{4\tau n_x^2} + \frac{\pi^2 k^2}{4\tau n_y^2}$, and if $n_x = n_y = n_s$, $n_s \gg 1$, and $j, k \ll n_s$, then the sum in (26) becomes

$$\sum_{m=1}^{n} \frac{1}{\omega^2 + \lambda_m^2} = \sum_{j,k=1}^{n_s} \frac{1}{\omega^2 + \lambda_{jk}^2}, \tag{B5}$$

$$\approx \int_{1/n_s}^{1-1/n_s} \int_{1/n_s}^{1-1/n_s} \frac{dxdy}{\omega^2 + \left(\frac{\pi^2 r^2}{4\tau}\right)^2}, \tag{B6}$$

$$\approx \frac{\pi}{2} \int_{\sqrt{2}/n_s}^{\sqrt{\xi}} \frac{rdr}{\omega^2 + \left(\frac{\pi^2 r^2}{4\tau}\right)^2}, \tag{B7}$$

$$\approx \frac{\pi}{4} \int_{2/n_s^2}^{\xi} \frac{dt}{\omega^2 + \left(\frac{\pi^2}{4\tau}\right)^2 t^2}, \tag{B8}$$

where $\frac{j}{n_s} \to x$, $\frac{k}{n_s} \to y$, $r^2 = x^2 + y^2$, and ξ is a number between 1 and 2 (and therefore $\xi \gg \frac{2}{n_s^2}$). The integral (B8) is just the integral (1) that leads to a $1/f$ PSD.

All this can be repeated for the 3D lattice using (51), and one finds that $|\lambda_{jkl}| \approx \frac{\pi^2 j^2}{6\tau n_x^2} + \frac{\pi^2 k^2}{6\tau n_y^2} + \frac{\pi^2 l^2}{6\tau n_z^2}$, and if $n_x = n_y = n_z = n_s$, $n_s \gg 1$, and $j, k, l \ll n_s$, then the sum in (26) becomes

$$\sum_{m=1}^{n} \frac{1}{\omega^2 + \lambda_m^2} = \sum_{j,k,l=1}^{n_s} \frac{1}{\omega^2 + \lambda_{jkl}^2}, \tag{B9}$$

$$\approx \int_{1/n_s}^{1-1/n_s} \int_{1/n_s}^{1-1/n_s} \int_{1/n_s}^{1-1/n_s} \times \frac{dxdydz}{\omega^2 + \left(\frac{\pi^2 r^2}{6\tau}\right)^2}, \tag{B10}$$

$$\approx \frac{\pi}{2} \int_{\sqrt{3}/n_s}^{\sqrt{\xi}} \frac{r^2 dr}{\omega^2 + \left(\frac{\pi^2}{6\tau}\right)^2 r^4}, \tag{B11}$$

$$\approx \frac{9\tau}{2\pi} \sqrt{\frac{\tau}{3}} \frac{1}{\omega^{1/2}}, \tag{B12}$$

where, once again, $\frac{j}{n_s} \to x$, $\frac{k}{n_s} \to y$, $\frac{l}{n_s} \to z$, $r^2 = x^2 + y^2 + z^2$, $1 < \xi < 3$, and $\lambda_{\min} \ll \omega \ll \lambda_{\max}$. The sum (B9) thus gives a $1/f^{0.5}$ PSD.

APPENDIX C

The space correlation function is easily computed using the formalism of Sec. III,

$$\langle (N_j^*(t) - \langle N_j \rangle_{\text{eq}}^*)(N_k(t) - \langle N_k \rangle_{\text{eq}}) \rangle = \frac{1}{(2\pi)^2} \int_{-\infty}^{+\infty} \int_{-\infty}^{+\infty} d\omega d\omega' e^{-i(\omega - \omega')t} \langle F_j^*(\omega) F_k(\omega') \rangle \tag{C1}$$

so that, using (22) and $\langle \gamma_l^*(\omega) \gamma_m(\omega') \rangle = \sigma^2 \delta_{lm} \delta(\omega - \omega')$,

$$\langle F_j^*(\omega) F_k(\omega') \rangle = \sigma^2 \sum_{l=1}^{n} \frac{(\boldsymbol{\eta}_l^*)_j (\boldsymbol{\eta}_l)_k}{\omega^2 - |\lambda_l|^2} \delta(\omega - \omega'), \tag{C2}$$

and thus the integral (C1) becomes

$$\langle (N_j^*(t) - \langle N_j \rangle_{\text{eq}}^*)(N_k(t) - \langle N_k \rangle_{\text{eq}}) \rangle = \frac{\sigma^2}{(2\pi)^2} \int_{-\infty}^{+\infty} d\omega \sum_{l=1}^{n} \frac{(\boldsymbol{\eta}_l^*)_j (\boldsymbol{\eta}_l)_k}{\omega^2 - |\lambda_l|^2} = \frac{\sigma^2}{4\pi} \sum_{l=1}^{n} \frac{(\boldsymbol{\eta}_l^*)_j (\boldsymbol{\eta}_l)_k}{|\lambda_l|}. \tag{C3}$$

In general the sum (C3) is different from zero, however this space correlation is not ruled out by past experiments. I review now the arguments of a few of them [25–27,23].

The experiment reported in [25] simply does not apply here, since it ruled out correlations in two gold films that were in thermal contact but electrically disconnected. The authors of [26] tried to measure voltage cross correlations in a thin wire that was etched, together with the contact pads, from a thin metal film. I argue here that they did not observe fluctuations *in the wire* but rather *in each pad separately*. In fact, whatever the (microscopic) origin of the fluctuations it must act in the pads as well as in the wire. If the explanation proposed in this paper has any validity at all, one should then expect the whole "wire + pads" system to behave — more or less — like a 2D system, and indeed what they observe is not the $1/f^{1.5}$ spectrum that was expected from

the Voss and Clark theory, but a $1/f$ spectrum which is characteristic of a 2D system (see Fig. 2 in [26]).

Again, the experiments reported in [27,23] test thermal fluctuations and do not apply here. Furthermore the observed dependence of noise power on sample width, which the authors of those papers used to argue that the noise arises from fluctuations in the local sheet resistivity, does not apply to number fluctuations and can be used instead to support formula (66), which does predict the observed dependence.

The averages (C2) are also proportional to the cross-spectra that appear in Eq. (62). I show here — for the 1D chain described at the beginning of Sec. V—that these terms have the same frequency dependence as the PSD.

The eigenvalues are given by Eq. (42), while the normalized eigenvectors are

$$(\boldsymbol{\eta}_m)_k = \sqrt{\frac{2}{n+1}} \sin \frac{\pi m k}{n+1}, \tag{C4}$$

therefore the sum in (C2) becomes

$$\sum_{l=1}^{n} \frac{(\boldsymbol{\eta}_l^*)_j (\boldsymbol{\eta}_l)_k}{\omega^2 - |\lambda_l|^2} = \left(\frac{2}{n+1}\right) \sum_{l=1}^{n} \frac{\sin \frac{\pi l j}{n+1} \sin \frac{\pi l k}{n+1}}{\omega^2 + \frac{1}{\tau^2}\left(1 - \cos \frac{\pi l}{n+1}\right)^2}. \tag{C5}$$

Introducing the auxiliary variable $x = \frac{\pi l}{n+1}$ and assuming $n \gg 1$, the sum (C5) can be approximated by the integral

$$\frac{\tau^2}{\pi} \int_0^{\pi} dx \frac{\cos[(j-k)x] - \cos[(j+k)x]}{(\omega\tau)^2 + (1-\cos x)^2}$$

$$\approx \frac{4\tau^2}{\pi} \int_0^{\infty} dx \frac{\cos[(j-k)x] - \cos[(j+k)x]}{(2\omega\tau)^2 + x^4}$$

for $x \ll 1$. The last integral can be evaluated with the help of formula (3.727.1) in [28], so that

$$\sum_{l=1}^{n} \frac{(\boldsymbol{\eta}_l^*)_j (\boldsymbol{\eta}_l)_k}{\omega^2 - |\lambda_l|^2} \approx \frac{\sqrt{\tau}}{2} \frac{1}{\omega^{3/2}} e^{-|j-k|\sqrt{\omega\tau}} \times \left(\cos|j-k|\sqrt{\omega\tau} + \sin|j-k|\sqrt{\omega\tau}\right), \tag{C6}$$

and therefore for sites that are not too far apart the cross terms (C2) have the same frequency dependence as the PSD (on the other hand the exponential terms "kill" the very contributions due to sites that are very far apart), so that the cross spectra have the same frequency dependence as the PSD.

[1] W. H. Press, Comments Astrophys. **7**, 103 (1978).

[2] B. J. West and M. Shlesinger, Int. J. Mod. Phys. **B3**, 795 (1989); Am. Sci. **78**, 40 (1990).

[3] M. Gardner, Sci. Am. **238**, 16 (1978).

[4] R. F. Voss and J. Clarke, Nature **258**, 317 (1975); J. Acoust. Soc. Am. **63**, 258 (1978).

[5] Sh. M. Kogan, Usp. Fiz. Nauk **145**, 285 (1985) [Sov. Phys. Usp. **28**, 170 (1985)].

[6] P. Dutta and P. M. Horn, Rev. Mod. Phys. **53**, 497 (1981).

[7] M. B. Weissman, Rev. Mod. Phys. **60**, 537 (1988).

[8] Here a "linear system" is whatever can be described by a set of variables $\boldsymbol{y} = \{y_i\}$ with the evolution equation $\dot{\boldsymbol{y}} = A\boldsymbol{y}$, where A is a real constant matrix. If $\boldsymbol{y}$ is a set of relaxing systems, A shall be called "relaxation matrix."

[9] R. F. Voss and J. Clarke, Phys. Rev. B **13**, 556 (1976).

[10] W. Feller, *An Introduction to Probability Theory and Its Applications*, third revised printing (Wiley, New York, 1968).

[11] We notice that the assumption $aN\Delta t \gg 1$ corresponds to the usual hypothesis of time scale separation required in the formulation of any Langevin equation The rationale for time scale separation is discussed in [21] and more recently in S. Sandow and S. Trimper, J. Phys. A **26**, 3079 (1993). In this respect we remark that forcing the stochastic term to be the high frequency part of the stochastic equation (6) is a perfect choice for a model of $1/f$ noise which is meant to study the low frequency components.

[12] D. R. Cox and H. D. Miller, *The Theory of Stochastic Processes* (Chapman and Hall, London, 1965).

[13] M. C. Wang and G. E. Uhlenbeck, Rev. Mod. Phys. **17**, 323 (1945); also in *Selected Papers on Noise and Stochastic Processes*, edited by N. Wax (Dover, New York, 1955).

[14] R. A. Horn and C. R. Johnson, *Matrix Analysis* (Cambridge University Press, Cambridge, 1987).

[15] F. Brauer and J. A. Nohel, *The Qualitative Theory of Ordinary Differential Equations* (Dover, New York, 1989).

[16] This is also clear if we take the sum (26) and use the Wiener-Kintchine theorem to evaluate the variance of the process.

[17] W. H. Press, S. A. Teukolsky, W. T. Vetterling, and B. P. Flannery, *Numerical Recipes in C, The Art of Scientific Computing, Second Edition* (Cambridge University Press, Cambridge, 1992).

[18] F. N. Hooge, T. G. M. Kleinpenning, and L. K. J. Vandamme, Rep. Prog. Phys. **44**, 479 (1981).

[19] S. H. Liu, Phys. Rev. B **16**, 4218 (1977); H. J. Jensen, Phys. Scr. **43**, 593 (1991); G. Grinstein, T. Hwa, and H. J. Jensen, Phys. Rev. A **45**, R559 (1992).

[20] H. van Beijeren, R. Kutner, and H. Spohn, Phys. Rev. Lett. **18**, 2026 (1985); H. F. Ouyang, Z. Q. Huang, and E. J. Ding, Phys. Rev. E **50**, 2491 (1994).

[21] N. G. van Kampen, *Stochastic Processes in Physics and Chemistry* (North-Holland, Amsterdam, 1981).

[22] V. Radeka, IEEE Trans. Nucl. Sci. **16**, 17 (1969).

[23] J. H. Scofield, J. V. Mantese, and W. W. Webb, Phys. Rev. B **32**, 736 (1985).

[24] J. W. Eberhard and P. M. Horn, Phys. Rev. B **18**, 6681 (1978).

[25] J. H. Scofield, D. H. Darling, and W. W. Webb, Phys. Rev. B **24**, 7450 (1981).
[26] R. D. Black, M. B. Weissman, and F. M. Fliegel, Phys. Rev. B **24**, 7454 (1981).
[27] D. M. Fleetwood, J. T. Masden, and N. Giordano, Phys. Rev. Lett. **50**, 450 (1983).
[28] I. S. Gradshteyn and I. M. Ryzhik, *Table of Integrals, Series and Products, Fourth Edition* (Academic Press, San Diego, 1990).